NJC

ROYAL SOCIETY OF CHEMISTRY

PAPER

View Article Online
View Journal | View Issue



Cite this: *New J. Chem.*, 2025, **49**, 7216

# Exploring the catalytic and anticancer activity of gold(I) complexes bearing 1,3,5-triaza-7-phosphaadamantane (PTA) and related ligands†

Nuno Reis Conceição, *[a] Abdallah G. Mahmoud, [bc] Martin C. Dietl, [d] Isabella Caligiuri,[e] Flavio Rizzolio, [ef] Sónia A. C. Carabineiro, *[ab] Matthias Rudolph,[d] M. Fátima C. Guedes da Silva, [ag] Armando J. L. Pombeiro, [a] A. Stephen K. Hashmi [d] and Thomas Scattolin *[h]

A series of water-soluble gold(I) complexes bearing phosphine ligands, [AuCl(L)] {where L = 1,3,5-triaza-7-phosphaadamantane, PTA (**1**); 3,7-diacetyl-1,3,7-triaza-5-phosphabicyclo[3.3.1]nonane, DAPTA (**2**); or 1,3,7-triaza-5-phosphabicyclo[3.3.1]nonane-3,7-diylbisphenylmethanone, DBPTA (**3**)} and [AuCl(L)]X {where L is either PTA-$CH_2$-$C_6H_4$-*p*-COOH and X = Br (**4**) or PTA-$CH_2$-$C_6H_3$-*p*-OH-*m*-CHO and X = Cl (**5**)}, were synthesized under mild conditions and characterized with multinuclear ($^1$H, $^{13}$C and $^{31}$P) nuclear magnetic resonance (NMR) spectroscopy, attenuated total reflection – Fourier transform infrared (ATR-FTIR) spectroscopy, matrix-assisted laser desorption/ionization – mass spectrometry (MALDI-MS) and elemental analysis. The catalytic activity of the complexes was evaluated in the peroxidative oxidation of cyclohexane to cyclohexanol and cyclohexanone. Homogeneous reactions were conducted in aqueous media, while heterogeneous reactions were performed after immobilizing the complexes on porous carbon supports, including activated carbon (AC), carbon nanotubes (CNT) and their oxidized derivatives (AC-ox, AC-ox-Na, CNT-ox and CNT-ox-Na). The results demonstrated a better catalytic performance, in terms of yields and selectivity, under heterogeneous conditions depending on the nature of the carbon support. Finally, complexes **1–5** showed remarkable cytotoxicity against a selection of ovarian, lung and colon cancer cell lines, with $IC_{50}$ values comparable to (or even better than) those of cisplatin. Interestingly, the most promising complexes exhibited good to excellent cytotoxicity against cancer cells while demonstrating substantial inactivity against normal ones.

Received 17th March 2025,
Accepted 3rd April 2025

DOI: 10.1039/d5nj01194a

rsc.li/njc



## 1. Introduction

The role of homogeneous gold-catalysed organic transformations has rapidly grown over the last two decades due to important characteristics, including high atom economy, remarkable tolerance for diverse functional groups, enhancement of molecular complexity and orthogonal reactivities when compared to alternative transition metal catalysts.[1–3] Gold catalysis in homogeneous media can exhibit high activity and enantioselectivity, with well-characterized structures facilitating the anticipation of mechanistic pathways.[4–7] On the other hand, heterogeneous gold catalysts offer advantages, such as longer lifetime, recyclability, ease of separation from the product and adaptability to continuous flow processes.[8–12] Therefore, the anchoring of soluble gold catalysts on solid supports has emerged as a promising interface area, combining the remarkable features of homogeneous catalysis with the benefits of heterogeneous systems.[13]

Various supports have been employed for the heterogenization of gold catalysts, including metal oxides,[14–16] organic

[a] *Centro de Química Estrutural, Institute of Molecular Sciences, Instituto Superior Técnico, Universidade de Lisboa, Av. Rovisco Pais, 1049-001 Lisboa, Portugal. E-mail: nunoconceicao@tecnico.ulisboa.pt*
[b] *LAQV-REQUIMTE, Department of Chemistry, NOVA School of Science and Technology, Universidade NOVA de Lisboa, 2829-516 Caparica, Portugal. E-mail: sonia.carabineiro@fct.unl.pt*
[c] *Department of Chemistry, Faculty of Science, Helwan University, Ain Helwan, Cairo 11795, Egypt*
[d] *Organisch-Chemisches Institut, Heidelberg University, Im Neuenheimer Feld 270, 69120 Heidelberg, Germany*
[e] *Pathology Unit, Department of Molecular Biology and Translational Research, Centro di Riferimento Oncologico di Aviano (CRO) IRCCS, via Franco Gallini 2, 33081, Aviano, Italy*
[f] *Dipartimento di Scienze Molecolari e Nanosistemi, Università Ca' Foscari, Campus Scientifico Via Torino 155, 30174 Venezia-Mestre, Italy*
[g] *Departamento de Engenharia Química, Instituto Superior Técnico, Universidade de Lisboa, Av. Rovisco Pais, 1049-001 Lisboa, Portugal*
[h] *Dipartimento di Scienze Chimiche, Università degli studi di Padova, via Marzolo 1, 35131, Padova, Italy. E-mail: thomas.scattolin@unipd.it*

† Electronic supplementary information (ESI) available. See DOI: https://doi.org/10.1039/d5nj01194a

 

polymers,[17] zeolites[18,19] and metal organic frameworks.[20,21] Porous carbon materials, such as activated carbon (AC) and carbon nanotubes (CNT), serve as exceptional carriers for catalytically active components due to their robust resistance to acids and alkalis, large surface area, low mass density and efficient mass transport.[22–24] Consequently, several recent studies have explored the heterogenization of Au complexes on porous carbon materials for various organic transformations, including oxidation of alkanes and alcohols,[25,26] cyclization of enynes[27,28] and hydroamination of alkynes.[29]

The hydrosoluble cage-like aminophosphine 1,3,5-triaza-7-phosphaadamantane (PTA) and its derivatives have attracted considerable interest in the field of organometallic chemistry with applications in catalysis, medicinal inorganic chemistry, photoluminescence and electrochemistry.[30–34] A substantial library of water-soluble complexes bearing PTA or its derivatives coordinated to group 11 metals (Cu, Ag and Au) through the P-atom has been reported.[30,32] However, the utilization of Au complexes bearing PTA ligands has been primarily limited to biological and photoluminescence applications.[30,34] The application of PTA complexes bearing coinage metals as catalysts for organic transformations has been confined to Cu only.[32,35–41]

Herein, we present the synthesis and characterization of a set of water-soluble Au(I) complexes bearing PTA and its *N*-diacylated and *N*-alkylated derivatives, namely 3,7-diacetyl-1,3,7-triaza-5-phosphabicyclo[3.3.1]nonane (DAPTA) 1,3,7-triaza-5-phosphabicyclo[3.3.1]nonane-3,7-diylbisphenylmethanone (DBPTA), (PTA-$CH_2$-$C_6H_4$-*p*-COOH)Br and (PTA-$CH_2$-$C_6H_3$-*p*-OH-*m*-CHO)Cl (Fig. 1), with [AuCl(DBPTA)] (**3**) and [AuCl(PTA-$CH_2$-$C_6H_3$-*p*-OH-*m*-CHO)]Cl (**5**) being novel compounds.

The obtained complexes were immobilized on carbon supports, along with their oxidized derivatives, to be used as efficient and recyclable catalysts for microwave-assisted oxidation of cyclohexane to cyclohexanol and cyclohexanone in an aqueous medium. To the best of our knowledge, this report is the first to study the catalytic properties of Au complexes bearing PTA-core ligands.

Since the serendipitous discovery of the antitumor properties of cisplatin,[42,43] many researchers in the fields of coordination and organometallic chemistry have actively contributed to the development of new potential metallodrugs for cancer therapy. Despite the advancements achieved with platinum complexes, which have led to the commercialization of well-established second- and third-generation platinum-based antineoplastic drugs (carboplatin and oxaliplatin),[44] their limited effectiveness against diverse tumour types or the emergence of drug resistance observed in many patients has spurred numerous scientists to explore the anticancer properties of complexes incorporating metals other than platinum.[45–48]

Among the various metal derivatives studied, gold(I) complexes hold a crucial place in medicinal chemistry, especially as therapeutic drugs for rheumatoid arthritis treatment.[49] Encouraging results regarding their effectiveness as antibiotics and anticancer agents have propelled several promising compounds into ongoing clinical trials.[50–56] Extensive research in recent decades has unveiled the diverse cellular targets of anticancer gold complexes, including mitochondria and

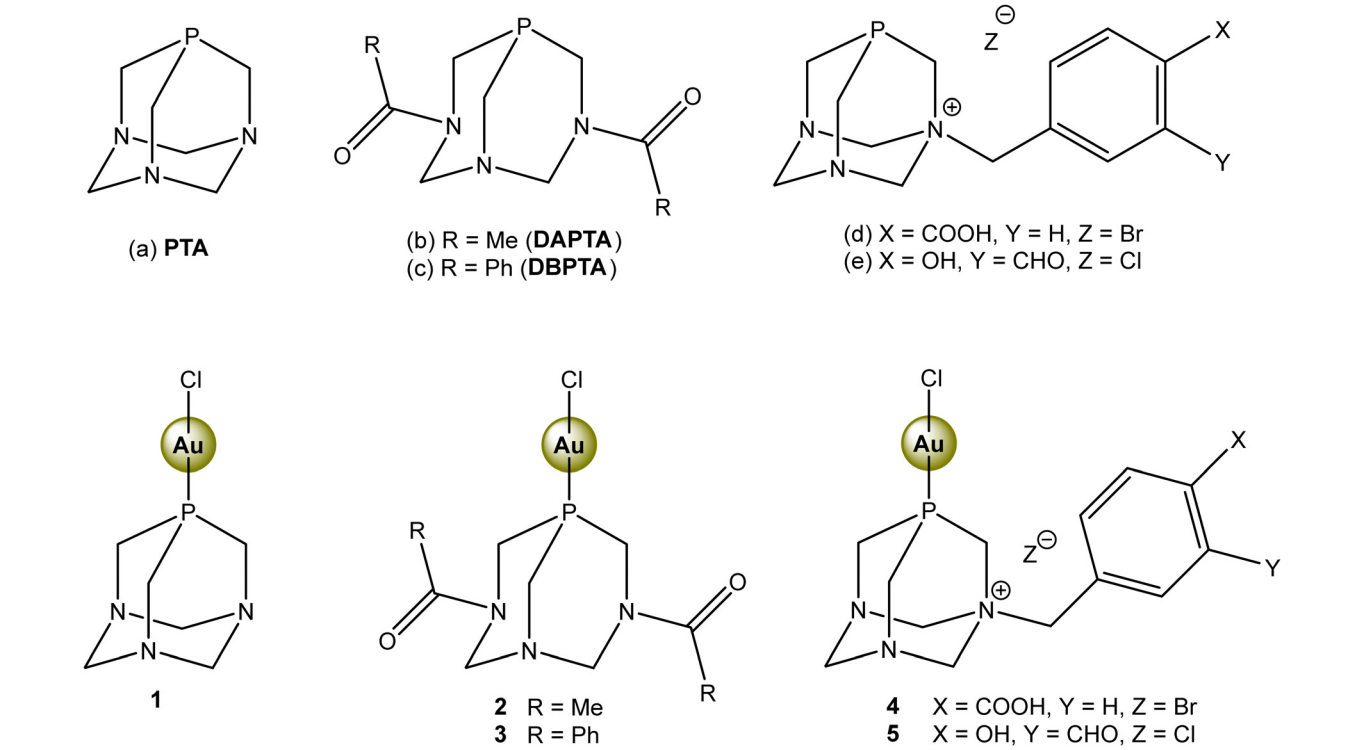


Fig. 1 Structures of the phosphine ligands and related gold(I) complexes employed in this study.

proteins with significant functional roles like thioredoxin reductase, poly(ADP-ribose) polymerase (PARP-1), cathepsins, proteasome, and protein tyrosine phosphatase.[50–56] Notably, pioneering studies by Mirabelli *et al.* on the 1-thio-β-D-(glucopyranose-2,3,4,6-tetraacetato-*S*)(triethylphosphine) gold(I) complex, known as auranofin, have induced the development of gold-based anticancer agents.[57] Initially introduced in the 1980s as an anti-arthritis medication, auranofin has recently gained FDA approval for phase II clinical trials in cancer therapy.[58]

In this paper, we also investigated the anticancer potential of the above-mentioned gold(I) complexes **1–5** by evaluating their cytotoxicity against various human cancer cell lines, including ovarian cancer (A2780 and its cisplatin-resistant variant A2780*cis*), colon cancer (HCT116), and lung cancer (A549), as well as normal human lung fibroblast cells (MRC-5). The antiproliferative activity was assessed through $IC_{50}$ values after 96 h of incubation, comparing the gold complexes with cisplatin as a reference.

## 2. Results and discussion

### 2.1. Synthesis and characterization of the Au(I) compounds

Five gold(I) complexes were synthesized by reacting [AuCl-($Me_2S$)] with phosphine ligands in either dichloromethane or acetone at room temperature. The neutral complexes [AuCl(L)] were obtained with L = PTA (**1**), DAPTA (**2**) or DBPTA (**3**). Cationic complexes [AuCl(L)]X were prepared with L = PTA-$CH_2$-$C_6H_4$-*p*-COOH and X = Br (**4**) or PTA-$CH_2$-$C_6H_3$-*p*-OH-*m*-CHO and X = Cl (**5**). All complexes were characterized using elemental analysis, multinuclear ($^1$H, $^{13}$C, and $^{31}$P) NMR (Fig. S1–S24, ESI†), ATR-FTIR (Fig. S25–S29, ESI†) and MALDI-MS.

The NMR spectra of **1** and **2** (Fig. S1–S8, ESI†) exhibited chemical shifts and splitting patterns consistent with those reported in the literature.[59,60] The $^{31}P\{^1H\}$ NMR resonances of **1** at −51.53 ppm and **2** at −26.74 ppm were downfield shifted relative to the corresponding free phosphines (−98 ppm for PTA and −78 ppm for DAPTA[30,37]), indicating successful coordination to the gold centre through P atom. In the $^1$H NMR spectrum of complex **2** (Fig. S5, ESI†), the presence of two distinct signals at 1.97–1.96 and 2.06–2.03 ppm suggested non-equivalence of the acetyl groups (*anti*-ZE configuration).[30,37] This was further confirmed by $^{13}C\{^1H\}$ NMR (Fig. S7, ESI†), which shows two sets of signals at 169.40 and 168.65 ppm (carbonyl carbons), and 21.58 and 21.27 (methyl carbons). The MALDI-MS spectra also confirm the successful synthesis of complexes **1** and **2**, with the detection of the molecular ion $[M]^+$ and/or related peaks ($[M - Cl]^+$, $[M + H]^+$ or $[M + Na]^+$). The ATR-FTIR spectra show a set of bands typical of the corresponding phosphine ligands (Fig. S25 and S26, ESI†), and a strong peak at 1633 $cm^{-1}$ was observed for compound **2**, which is attributed to the carbonyl group stretching vibration.

The novel [AuCl(DBPTA)] compound (**3**) exhibits peak patterns and chemical shifts in the $^1$H and $^{13}C\{^1H\}$ NMR spectra (Fig. S9–S12, ESI†) consistent with those reported for the uncoordinated phosphine.[38] The coordination of DBPTA to the Au(I) centre is further confirmed by the downfield shift of its $^{31}P\{^1H\}$ NMR signal from −77.36 to −24.53 ppm. The benzoyl groups in **3** are magnetically inequivalent (*anti*-ZE orientation),[38] as evidenced by $^{13}C\{^1H\}$ NMR spectra (Fig. S11, ESI†) with the presence of two distinct set of signals attributed to C=O (at 169.98 and 169.48 ppm) and $C_{quat}$–CO (at 134.64 and 134.57 ppm). The IR spectrum of **3** (Fig. S27, ESI†) exhibits a strong peak at 1631 $cm^{-1}$, associated with the C=O stretching vibration, along with several medium-intensity peaks resembling those of the free ligand.[38] The detection of the $[M + Na]^+$ ion in the MALDI-MS spectra provides further evidence of the successful synthesis of [AuCl(DBPTA)].

The NMR spectra (Fig. S13–S18, ESI†) of [AuCl(PTA-$CH_2$-$C_6H_4$-*p*-COOH)]Br (**4**) show chemical shifts and peak splitting patterns consistent with literature reports for this compound.[61] The signal observed in the $^{31}P\{^1H\}$ NMR spectrum (Fig. S14, ESI†) at −30.83 ppm was downfield shifted when compared to the free phosphine ligand at −83.40 ppm[41] due to the coordination to the Au centre.[61] The MALDI-MS spectra display two peaks corresponding to the molecular ion ($[M - Cl]^+$ and $[M + H]^+$) while the ATR-FTIR spectrum (Fig. S28, ESI†) exhibits an intense band at 1698 $cm^{-1}$ (C=O stretching), which is close to the frequency reported in the literature (1721 $cm^{-1}$).[61]

The new gold(I) complex [AuCl(PTA-$CH_2$-$C_6H_3$-*p*-OH-*m*-CHO)]Cl (**5**) was also characterized through NMR spectroscopy (Fig. S19–S24, ESI†). The $^1$H NMR spectrum (Fig. S19, ESI†) exhibited characteristic resonances for the hydroxyl (11.44 ppm) and the formyl (10.34 ppm) functional groups. Aromatic proton signals were observed in the range of 7.8–7.2 ppm, while a set of signals between 5.3–4.2 ppm correlated to the diastereotopic methylene protons of the PTA cage.[41] The $^{31}P\{^1H\}$ NMR spectrum of **5** (Fig. S20, ESI†) displays a prominent signal at −32.17 ppm, significantly downfield-shifted from the free ligand (−83.72 ppm).[41] The IR spectrum (Fig. S29, ESI†) reveals two strong peaks at 1687 and 1661 $cm^{-1}$, attributed to the carbonyl group stretching, and other two additional peaks at 816 and 743 $cm^{-1}$, corresponding to the =C–H bending vibrations. The MALDI-MS spectrum show the molecular ion $[M]^+$ peak along with the associated peaks $[M - Cl]^+$ and $[M + Na]^+$.

### 2.2. Heterogenization process

The gold complexes were heterogenized onto the different carbon materials: the original forms (AC and CNT), oxidized with refluxing 7 M nitric acid (-ox), and oxidized with $HNO_3$ followed by treatment with refluxing 20 mM NaOH (-ox-Na), according to procedures described in previous publications.[23–26,38,39] These supports were able to anchor the gold complexes, achieving the desired loading of approximately 2% Au, although with varying efficiencies, as assessed by inductively coupled plasma (ICP) analysis. The CNT materials (Fig. S45–S59, ESI†) exhibited the highest efficiency after 1 to 4 h of stirring at room temperature, with the exception of **5**@CNT-ox-Na, which required 24 h. The AC materials (Fig. S30–S44, ESI†) showed a heterogenization efficiency slightly lower than that of CNTs, achieving the required Au loading after 24 h (exception for the non-oxidized AC supports,

 

which demand a longer process). In general, the gold(I) complexes were more effectively heterogenized on the oxidized supports when compared to the pristine ones, likely due to the increased number of surface groups available for anchoring, resulting from the functionalization of the carbon materials.[25,62–64] This result is consistent with findings from other studies on the heterogenization of gold(I) and/or gold(III) compounds onto similar carbon supports.[25,26]

### 2.3. Catalytic reactions

The catalytic activity of gold complexes **1–5** was evaluated in the oxidation of cyclohexane to cyclohexanone and cyclohexanol (known as KA oil, Scheme 1). Reactions were conducted using *tert*-butyl hydroperoxide (TBHP, 70% aqueous solution) as the oxidant in acetonitrile at 50 °C for 4 hours, with 0.15 mol% of the gold(I) catalyst, nitric acid as a promoter, and AgOTf as an activating agent (by replacing the chloride ligand with the more labile triflate anion, $OTf^-$, through precipitation of AgCl).

Only complexes **1** and **5** exhibited catalytic activity, producing cyclohexanol with low yields of 0.2% and 0.4%, respectively (Table 1, entries 1 and 3). Complex **4** displayed activity when hydrogen peroxide was used as oxidant instead of TBHP, also affording cyclohexanol with a 0.3% yield (Table 1, entry 2). Increasing the loading of catalyst **1** to 1 mol% slightly improved the cyclohexanol yield to 0.3 and 0.4% using $H_2O_2$ and TBHP, respectively (Table 1, entries 4 and 5). The reaction was also performed using catalyst **1** under microwave irradiation at 70 °C to produce the alcohol with 0.5% yield after only 30 min (Table 1, entry 6). The use of the gold precursor [AuCl($Me_2S$)] resulted in the formation of both cyclohexanol and cyclohexanone with yields of 0.1 and 0.7%, respectively (Table 1, entry 7). While the gold precursor exhibited slightly higher overall product yields (0.8%), with cyclohexanone as the major product, the gold complexes (**1**, **4**, and **5**) demonstrated selectivity towards cyclohexanol production.

Variations in reaction parameters, including the temperature (50–80 °C) and the type of promotor (nitric acid, pyridine and pyrazine-2-carboxylic acid), did not improve the catalytic performance in terms of the obtained yield. The oxidation of cyclohexane did not proceed in the absence of gold catalysts.

The catalytic activity of immobilized gold(I) complexes **1–5** was also investigated for cyclohexane oxidation. Under microwave irradiation, cyclohexane was oxidized with TBHP in acetonitrile at 50 °C for 30 min, in the presence of the heterogenous catalysts (0.15 mol% of the supported gold complex), nitric acid promoter and AgOTf activator. The results, summarized in Table 2, showed that all immobilized catalysts exhibited varying degrees of activity towards the oxidation reaction, including complexes **2** and **3** which were not active under homogeneous conditions.

Table 1 Catalytic performance of Au(I) complexes **1–5** in the peroxidative oxidation of cyclohexane in homogeneous aqueous medium[a]

| | | Yield[b] (%) | | | | |
|---|---|---|---|---|---|---|
| Entry | Compound | CyOH | Cy′O | Total | TON[c] | TOF[d]/$h^{-1}$ |
| 1 | **1** | 0.2 | — | 0.2 | 1.3 | 0.3 |
| 2[e] | **4** | 0.3 | — | 0.3 | 2.0 | 0.5 |
| 3 | **5** | 0.4 | — | 0.4 | 2.7 | 0.7 |
| 4[ef] | **1** | 0.3 | — | 0.3 | 0.3 | 0.1 |
| 5[f] | **1** | 0.4 | — | 0.4 | 0.4 | 0.1 |
| 6[g] | **1** | 0.5 | — | 0.5 | 3.3 | 6.6 |
| 7 | [AuCl($Me_2S$)] | 0.1 | 0.7 | 0.8 | 5.3 | 1.3 |

[a] Reaction conditions: cyclohexane (1 mmol), catalyst (1.5 μmol), AgOTf (1.5 or 3 μmol), TBHP (5 mmol), $HNO_3$ (25 μmol), and nitromethane (1 mmol), in acetonitrile and water, at 50 °C for 4 h. [b] Determined by GC. [c] Turnover number (moles of product per mole of catalyst). [d] Turnover frequency (TON per hour). [e] aq. $H_2O_2$ used as an oxidant (5 mmol). [f] 10 μmol of catalyst used. [g] Reaction performed under MW irradiation (70 °C) for 0.5 h.

When immobilized on AC and its oxidized derivatives, the gold(I) complexes exhibited catalytic behaviour similar to that observed in homogeneous solution in terms of selectivity (exclusive formation of cyclohexanol) and yields up to 0.6% were obtained (Table 2, entries 1–15). In contrast, immobilization on CNTs led to a significant shift in product selectivity. Cyclohexanone was selectively obtained, and higher yields were achieved, reaching a maximum of 6.8% (Table 2, entries 16–30).

Several factors may contribute to the enhanced catalytic performance observed when using CNTs supports. These include the textural properties (Table S1, ESI†), such as high pore volume and pore accessibility, which facilitate efficient reactant diffusion to the active sites. Additionally, the electronic properties of CNTs, particularly their graphitic structure, may influence the interaction between the support and the hydrophobic reaction components, potentially enhancing the catalytic activity.[25,26]

Oxidized CNTs (CNT-ox and CNT-ox-Na) generally exhibit improved catalytic performance due to their increased surface functionality. The introduction of oxygen-containing groups, such as phenols and carboxylates, that can act as coordination sites for the complexes creates potential anchoring sites for the

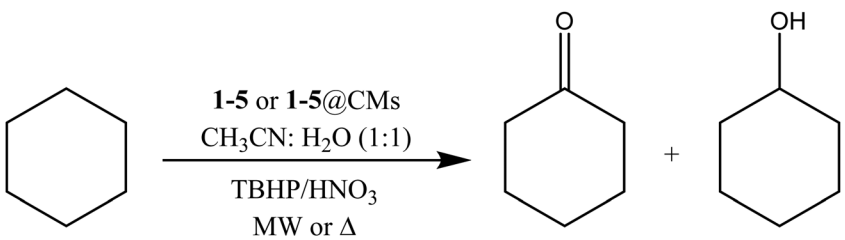


Scheme 1 Catalytic oxidation of cyclohexane to cyclohexanone and cyclohexanol.

Table 2 Catalytic performance of Au(I) complexes **1–5** supported on porous carbon materials in the cyclohexane oxidation under MW irradiation[a]

| Entry | Compound | Yield[b]/% | | | TON[c] | TOF[d]/h$^{-1}$ |
|---|---|---|---|---|---|---|
| | | CyOH | Cy′O | Total | | |
| 1 | **1**@AC | 0.5 | — | 0.5 | 3.3 | 6.6 |
| 2 | **1**@AC-ox | 0.2 | — | 0.2 | 1.3 | 2.6 |
| 3 | **1**@AC-ox-Na | 0.1 | — | 0.1 | 0.7 | 1.4 |
| 4 | **2**@AC | 0.6 | — | 0.6 | 4.0 | 8.0 |
| 5 | **2**@AC-ox | 0.2 | — | 0.2 | 1.3 | 2.6 |
| 6 | **2**@AC-ox-Na | 0.1 | — | 0.1 | 0.7 | 1.4 |
| 7 | **3**@AC | 0.5 | — | 0.5 | 3.3 | 6.6 |
| 8 | **3**@AC-ox | 0.1 | — | 0.1 | 0.7 | 1.4 |
| 9 | **3**@AC-ox-Na | 0.1 | — | 0.1 | 0.7 | 1.4 |
| 10 | **4**@AC | 0.6 | — | 0.6 | 4.0 | 8.0 |
| 11 | **4**@AC-ox | 0.1 | — | 0.1 | 0.7 | 1.4 |
| 12 | **4**@AC-ox-Na | 0.1 | — | 0.1 | 0.7 | 1.4 |
| 13 | **5**@AC | 0.5 | — | 0.5 | 3.3 | 6.6 |
| 14 | **5**@AC-ox | 0.1 | — | 0.1 | 0.7 | 1.4 |
| 15 | **5**@AC-ox-Na | 0.1 | — | 0.1 | 0.7 | 1.4 |
| 16 | **1**@CNT | — | — | — | — | — |
| 17 | **1**@CNT-ox | — | 2.7 | 2.7 | 18 | 36 |
| 18 | **1**@CNT-ox-Na | — | — | — | — | — |
| 19 | **2**@CNT | — | 4.3 | 4.3 | 28.7 | 57.4 |
| 20 | **2**@CNT-ox | — | 4.1 | 4.1 | 27.3 | 54.6 |
| 21 | **2**@CNT-ox-Na | — | 4.6 | 4.6 | 30.7 | 61.4 |
| 22 | **3**@CNT | — | 1.7 | 1.7 | 11.3 | 22.6 |
| 23 | **3**@CNT-ox | — | — | — | — | — |
| 24 | **3**@CNT-ox-Na | — | — | — | — | — |
| 25 | **4**@CNT | — | — | — | — | — |
| 26 | **4**@CNT-ox | — | 1.4 | 1.4 | 9.3 | 18.6 |
| 27 | **4**@CNT-ox-Na | — | 4.9 | 4.9 | 32.7 | 65.4 |
| 28 | **5**@CNT | — | — | — | — | — |
| 29 | **5**@CNT-ox | — | 6.8 | 6.8 | 45.3 | 90.6 |
| 30 | **5**@CNT-ox-Na | — | — | — | — | — |

[a] Reaction conditions: cyclohexane (1 mmol), catalyst (1.5 μmol supported on the carbon material), AgOTf (1.5 or 3 μmol), TBHP (5 mmol), $HNO_3$ (25 μmol) and nitromethane (1 mmol), in acetonitrile and water, at 50 °C for 0.5 h. [b] Determined by GC. [c] Turnover number (moles of product per mole of catalyst). [d] Turnover frequency (TON per hour).

catalyst, leading to more effective immobilization and, consequently, higher catalytic activity.[25,26,62–64]

No oxygenated products were detected upon separation and reuse of the heterogeneous catalysts in a second cycle, suggesting the decomposition of the Au(I) catalysts. This observation is further supported by a colour change of the solution from colourless to violet, most likely due to the formation of $Au^{3+}$ ions, after the first catalytic cycle.

**Comparison with other gold catalytic systems.** When compared to other reported gold-based catalysts, the catalytic system in this study demonstrates lower overall activity in terms of oxygenated product yields.

Homogeneous catalysis with Au(I)–phosphine complexes, namely [AuCl($PMe_3$)] and [AuCl($PPh_3$)], using TBHP as the oxidant, yielded KA oil in 1.7% after 6 h.[26] Supporting these complexes on AC and CNT materials improved their catalytic efficiency to obtain KA oil with yields up to 16.2% under heterogenous conditions.[26]

Furthermore, Au(III) complexes based on trispyrazolylmethane ligands demonstrated promising results in the cyclohexane oxidation with $H_2O_2$, achieving KA oil yields of up to 10.3% under homogeneous conditions and 16% when supported on oxidized CNT-ox-Na after 6 h.[25] Another gold(III) catalyst, [Au(phen)$Cl_2$]$NO_3$, exhibited a remarkable catalytic performance in the oxidation of cyclohexane by TBHP, yielding 45% of KA oil after 36 h.[65]

However, the catalytic system comprising the Au(I) complexes with PTA and related ligands exhibits a significant advantage of high selectivity towards either cyclohexanol or cyclohexanone, depending on the choice of carbon support material. Moreover, the utilization of microwave (MW) irradiation significantly enhances the reaction rate, achieving a maximum yield of 6.8% within 30 min at a mild temperature of 50 °C.

**Reaction mechanism.** The peroxidative oxidation of cyclohexane catalysed by Au(I) complexes **1–5** is proposed to occur primarily *via* a radical mechanism involving both carbon- and oxygen-centred radicals,[25,66] similar to processes observed in various $M^{n+1/n}$ systems (namely Cu,[41,67–72] also from group 11). The initial step involves the reduction of the oxidant by the Au(I) species, generating the *tert*-butoxyl radical ($^t$BuO$^\bullet$, eqn (1)), which abstracts a hydrogen atom from cyclohexane to generate the cyclohexyl radical (Cy$^\bullet$, eqn (3)). Cy$^\bullet$ is then oxidized by molecular oxygen to form the peroxyl radical (CyOO$^\bullet$, eqn (4)). This radical is reduced by Au(I) species, followed by protonation, leading to the formation of cyclohexyl hydroperoxide (CyOOH) as the primary product (eqn (5) and (6)). The formation of the alkoxyl (CyO$^\bullet$) and alkylperoxyl (CyOO$^\bullet$) radicals occurs through a metal-assisted decomposition of CyOOH (eqn (7) and (8)). These radicals are then converted into the alcohol (*via* substrate H-abstraction in eqn (9)) and the KA oil mixture (through dismutation in eqn (10)).

$$[Au^I] + {}^tBuOOH \rightarrow {}^tBuO^\bullet + [Au^{II}] + HO^- \quad (1)$$

$$[Au^{II}] + {}^tBuOOH \rightarrow {}^tBuOO^\bullet + H^+ + [Au^I] \quad (2)$$

$${}^tBuO^\bullet + CyH \rightarrow {}^tBuOH + Cy^\bullet \quad (3)$$

$$Cy^\bullet + O_2 \rightarrow CyOO^\bullet \quad (4)$$

$$CyOO^\bullet + [Au^I] \rightarrow CyOO^- + [Au^{II}] \quad (5)$$

$$CyOO^- + H^+ \rightarrow CyOOH \quad (6)$$

$$CyOOH + [Au^I] \rightarrow CyO^\bullet + HO^- + [Au^{II}] \quad (7)$$

$$CyOOH + [Au^{II}] \rightarrow CyOO^\bullet + H^+ + [Au^I] \quad (8)$$

$$CyO^\bullet + CyH \rightarrow CyOH + Cy^\bullet \quad (9)$$

$$2CyOO^\bullet \rightarrow CyOH + Cy'O + O_2 \quad (10)$$

However, the involvement of gold oxo or peroxo complexes as the oxidizing species should also be considered, suggesting a high-valent metal-oxo (HVMO) pathway,[73] in addition to the radical mechanism.

The use of an acetonitrile/water mixture is advantageous for dissolving both the substrate and catalyst. The choice of $CH_3CN$ is based on: (i) its miscibility with $H_2O$ and ability to dissolve the substrate, catalysts and products; (ii) its high stability under the oxidative conditions used; and (iii) its successful use in previously studied systems. The role of $HNO_3$ as a co-catalyst may be linked to: (i) promoting $H^+$-transfer steps; (ii) activating

 

Table 3 Antiproliferative activity of complexes **1–5** towards A2780, A2780*cis*, HCT116, A549, MRC-5 cell lines

| | $IC_{50}$[a]/μM | | | | |
|---|---|---|---|---|---|
| Compound | A2780 | A2780*cis* | HCT116 | A549 | MRC-5 |
| cisplatin | 1.1 ± 0.1 | 11 ± 3 | 21 ± 7 | 9 ± 1 | 2 ± 1 |
| **1** | 0.22 ± 0.08 | 22 ± 2 | 0.15 ± 0.03 | 21 ± 5 | 5 ± 1 |
| **2** | 0.29 ± 0.06 | 8 ± 2 | 0.24 ± 0.06 | 31 ± 9 | >100 |
| **3** | 0.26 ± 0.05 | 58 ± 20 | 0.16 ± 0.05 | >100 | >100 |
| **4** | 0.27 ± 0.07 | 3.4 ± 0.3 | 0.3 ± 0.1 | 19 ± 5 | >100 |
| **5** | 0.23 ± 0.08 | 54 ± 10 | 0.3 ± 0.1 | 27 ± 1 | >100 |

[a] Data after 96 h of incubation. Stock solutions in DMSO for all complexes; stock solutions in $H_2O$ for cisplatin. A2780 (cisplatin-sensitive ovarian cancer cells), A2780*cis* (cisplatin-resistant ovarian cancer cells), HCT116 (colon cancer cells), A549 (lung cancer cells), MDA-MRC-5 (lung fibroblasts).

the catalyst by causing unsaturation of the metal centre upon ligand protonation; (iii) enhancing the oxidative properties of the catalyst and the oxidant; and (iv) facilitating the formation of peroxo complexes.[74]

### 2.4. Anticancer activity of gold complexes 1–5

As stated in the introduction section, gold-based compounds are promising anticancer agents with mechanisms distinct from conventional chemotherapy. Unlike platinum-based drugs that primarily target DNA, gold compounds interact with proteins involved in redox regulation and cellular defense, such as thioredoxin reductase (TrxR).[49–56] Gold(I) and gold(III) complexes exhibit selective cytotoxicity against cancer cells by disrupting essential biomolecular functions. TrxR inhibition by gold complexes leads to oxidative stress and apoptosis, offering a targeted approach for cancer therapy.[75–77]

Moreover, the combination of gold complexes with conventional chemotherapeutic agents or targeted therapies can enhance anticancer efficacy through synergistic effects.[78,79] Gold complexes can sensitize cancer cells to existing drugs by modulating redox balance, inhibiting key enzymes, or disrupting cellular defense mechanisms. For instance, co-administration of gold-based compounds with platinum drugs has been shown to enhance DNA damage and apoptosis.[78] Additionally, gold complexes targeting TrxR or proteasomes can work in tandem with kinase inhibitors or immune checkpoint inhibitors, improving treatment outcomes.[79,80] The combination strategy not only reduces drug resistance but also allows for lower dosages, minimizing side effects.

With the aim of investigating the potential anticancer effects of the gold(I) complexes **1–5** synthesized in this study, various human tumour cell lines (including ovarian cancer A2780 and its cisplatin-resistant variant A2780*cis*, colon cancer HCT116, lung cancer A549) and normal cells (MRC-5 lung fibroblasts) were exposed to a 96-hour treatment with both the gold compounds and cisplatin (utilized as a positive control).

Initially, the stability of the complexes in a 1 : 1 $D_2O$/DMSO-$d_6$ solution was evaluated using NMR spectroscopy. After 24 h, no significant changes were observed in the spectra, indicating the structural integrity of the complexes.

The antiproliferative activity of the tested compounds is summarized in Table 3, which presents the half inhibitory concentrations ($IC_{50}$) values.

Gratifyingly, all compounds exhibit good to excellent antiproliferative activity across all tumour lines examined, with most $IC_{50}$ values falling within the micro- and submicromolar range.

Notably, all five compounds are more active than cisplatin, by up to one order of magnitude, against A2780 (cisplatin-sensitive ovarian cancer) and HCT116 (colon cancer) cell lines. However, when tested on the cisplatin-resistant A2780*cis* ovarian cancer cells, only complexes **2** and **4** exhibit superior activity compared to cisplatin. For A549 lung cancer cells, complex **3** appears to be inactive, while the other gold complexes exhibit slightly lower cytotoxicity than cisplatin.

In the MRC-5 non-tumour cell line, cisplatin shows a very low $IC_{50}$ of 2 μM, which is nearly identical to the values observed in the four cancer cell lines, highlighting the poor selectivity of this reference drug. In contrast, most of our gold complexes are inactive against normal cells ($IC_{50}$ > 100 μM), suggesting an intriguing *in vitro* selectivity for cancer cells.

Overall, complex **4** emerges as the most promising derivative, as it demonstrates the lowest $IC_{50}$ values against cancer cells while maintaining substantial inactivity towards normal ones. This indicates its potential for selective anticancer activity with minimal toxicity to healthy tissue, making it a strong candidate for further investigation.

## 3. Conclusions

In this study, gold(I) complexes **1–5** were synthesized by reacting the gold precursor [AuCl($Me_2S$)] with five phosphine ligands: PTA, DAPTA, DBPTA, (PTA-$CH_2$-$C_6H_4$-*p*-COOH)Br and (PTA-$CH_2$-$C_6H_3$-*p*-OH-*m*-CHO)Cl. The novel compounds, [AuCl(DBPTA)] (**3**) and [AuCl(PTA-$CH_2$-$C_6H_3$-*p*-OH-*m*-CHO)]Cl (**5**), as well as the ones bearing PTA (**1**), DAPTA (**2**) or PTA-$CH_2$-$C_6H_4$-*p*-COOH (**4**) ligands, were thoroughly characterized by elemental analysis, ATR-FTIR, multi-nuclear ($^1H$, $^{13}C$ and $^{31}P$) NMR and MALDI-MS.

These complexes were tested as potential catalysts in the peroxidative oxidation of cyclohexane in $CH_3CN/H_2O$ under mild conditions (conventional heating at 50 °C for 4 h or MW irradiation at 50 °C for 0.5 h). CyOH was selectively obtained with yields up to 0.5% using catalyst **1** upon addition of AgOTf as activator, TBHP as oxidant and $HNO_3$ as promoter, under homogenous conditions.

The immobilization of the Au(I) complexes on carbon supports (AC or CNT), pristine or oxidized (-ox and -ox-Na), improved their catalytic performance. Although the best result achieved with **5**@CNT-ox (6.8% of cyclohexanone) is below the ones reported for other gold compounds, we observed an interesting selectivity towards cyclohexanol or cyclohexanone that depends on the nature of the carbon support.

It is well-known that metal complexes immobilized in carbon nanotubes (CNTs) offer significant benefits in catalytic applications by enhancing efficiency, stability, and reusability.[81,82] Their high surface area improves catalytic activity by facilitating better

dispersion and interaction with reactants. Immobilization within CNTs usually prevents catalyst deactivation and leaching, ensuring prolonged durability. Additionally, CNT-supported catalysts are easily recoverable, making them more cost-effective and sustainable.

Finally, functionalization of CNTs allows for precise tuning of catalytic properties, optimizing reactivity and selectivity. These catalysts also contribute to greener chemistry by reducing metal waste and energy consumption.

The Au(I) complexes **1–5** were also tested against various cancer cell lines, including ovarian (A2780, A2780*cis*), colon (HCT116) and lung (A549) cancer cell lines, as well as normal human lung fibroblasts (MRC-5). These complexes demonstrated $IC_{50}$ values comparable, or even superior, to cisplatin. Notably, complexes **2–5** exhibited good to excellent cytotoxicity against cancer cells while showing minimal activity against normal cells, indicating promising selective anticancer potential.

Based on these encouraging results, further *in vitro* and *in vivo* studies, along with comprehensive mechanistic investigations, are currently underway in our laboratories to explore the full potential of these gold(I) complexes as therapeutic agents.

# 4. Experimental

## 4.1. General procedures

All reagents and solvents (p.a. grade) were obtained from commercial sources and used as received, including acetone (≥99.5%, Sigma-Aldrich); acetonitrile (≥99.9%, Fisher Chemical); dichloromethane (≥99.9%, Sigma-Aldrich); diethyl ether (≥99.5%, Fisher Scientific); dimethyl sulfoxide (DMSO) (≥99.9%, Sigma-Aldrich); methanol (≥99.8%, Fisher Scientific); *n*-pentane (9%, Fisher Scientific); cyclohexane (>99.5%, TCI); cyclohexanone (99.8%, Aldrich); cyclohexanol (99%, Aldrich); nitric acid (aqueous solution ≥65%, Sigma-Aldrich); pyridine (99.94%, Fisher Chemical); pyrazine-2-carboxylic acid (PCA) (>98%, TCI); hydrogen peroxide (aqueous solution 50%, Acros Organics); *tert*-butyl hydroperoxide (aqueous solution 70%, Acros Organics); nitromethane (>98%, Alfa Aesar); triphenylphosphine (99%, Acros Organics); silver(I) nitrate (≥99.0%, Sigma-Aldrich); silver(I) trifluoromethanesulfonate (or triflate) (≥99%, Aldrich).

Ligands PTA,[83] DAPTA,[84] DBPTA,[38] (PTA-$CH_2$-$C_6H_4$-*p*-COOH)Br[61] and (PTA-$CH_2$-$C_6H_3$-*p*-OH-*m*-CHO)Cl[41] were obtained using the reported procedures. The gold(I) precursor complex [AuCl($Me_2S$)] was synthesized following the published protocol.[85]

For the characterization of the gold(I) complexes through nuclear magnetic resonance (NMR), Bruker Avance III 400 (400 MHz) and Bruker Avance III 600 (600 MHz) spectrometers were employed. High-resolution mass spectra (HR-MS) were recorded on the following spectrometers: Bruker ApexQe hybrid 9.4 T FT-ICR and Bruker AutoFlex Speed (matrix-assisted laser desorption/ionization – mass spectrometry, MALDI-MS). Infrared spectra were recorded from a neat powder or oil on a Fourier transform – infrared (FT-IR) spectroscopy spectrometer Bruker LUMOS with a Germanium attenuated total reflectance (ATR) crystal; the most significant bands are reported in terms of their wave numbers. Elemental Analysis was performed on a Thermo Finnigan CE Instruments Flash EA 1112 CHNS analyser (with services provided by REQUIMTE Analysis Laboratory).

For the monitoring of the Au(I) complex heterogenization process on the carbon supports, a Lambda 35 ultraviolet/visible (UV/Vis) spectrometer from PerkinElmer was employed.

The microwave (MW) assisted experiments were performed on a microwave Anton Paar Monowave 300 reactor (10 W) fitted with a rotational system and an infrared (IR) temperature detector.

Quantitative analysis of the reaction mixtures was carried out using PerkinElmer Clarus 500 and 590 gas chromatographs equipped with BP-20 capillary columns (SGE; 30 m × 0.22 mm × 0.25 μm) and FID detectors. Helium was used as the carrier gas and the injector temperature was set to 200 °C.

## 4.2. Synthesis of the Au(I) complexes

The syntheses of Au(I) complexes [AuCl(PTA)] (**1**), [AuCl(DAPTA)] (**2**) and [AuCl(PTA-$CH_2$-$C_6H_4$-p-COOH)]Br (**4**) followed protocols based on established methods,[61,63,64] with several modifications including the utilization of a different gold precursor, different solvents, and performing the reactions in a normal atmosphere instead of an inert one.

**[AuCl(PTA)] (1).** In a small flask equipped with a magnetic stirring bar, [AuCl($Me_2S$)] (0.17 mmol, 50 mg) was dissolved in 1 mL of dichloromethane (DCM) and a solution of PTA (0.17 mmol, 26.7 mg) in 1.5 mL of DCM was added dropwise. The resulting mixture was stirred at room temperature (r.t.) for 2 h and approximately 1 mL of *n*-pentane was added afterwards. The capped flask was then stored at −32 °C overnight. The colourless precipitate formed was filtered and washed with portions of *n*-pentane. The volume of the filtrate was reduced using a rotary evaporator to obtain more quantity of the compound, which was also filtered and dried under vacuum.

Yield = 87% (57.5 mg) based on the metal salt. Elemental analysis calcd (%) for $C_6H_{12}AuClN_3P$: C 18.50, H 3.10, N 10.79; found: C 19.93, H 3.07, N 10.97. ATR-FTIR, $\nu$ ($cm^{-1}$): 2909 w, 2873 w, 1446 w, 1417 w, 1279 m, 1242 s, 1097 m, 1040 w, 1012 s, 973 vs, 946 vs, 898 m, 809 m, 740 vs, 659 w. $^1$H NMR (400 MHz, DMSO-$d_6$), $\delta$ (ppm): 4.51 (d, $^2J_{HH}$ = 8.4 Hz, 3H, NC$H_{2(ax)}$N), 4.38 (d, $^2J_{HH}$ = 8.4 Hz, 3H, NC$H_{2(eq)}$N), 4.32 (s, 6H, PC$H_2$N). $^{31}$P{$^1$H} NMR (400 MHz, DMSO-$d_6$), $\delta$ (ppm): −51.53. $^{13}$C{$^1$H} NMR (400 MHz, DMSO-$d_6$), $\delta$ (ppm): 71.76 (N$CH_2$N), 50.70 (d, $^1J_{PC}$ = 64 Hz, P$CH_2$N). DEPT (400 MHz, DMSO-$d_6$), $\delta$ (ppm): 71.41, 50.37. MALDI-MS (DCTB matrix), *m*/*z* (assignment, % intensity): 743 ([M + Au{PTA}]$^+$, 6), 390 ([M + H]$^+$, 0.7), 374 ([Au{PTA} + $H_2O$]$^+$, 100), 354 ([M − Cl]$^+$, 2).

**[AuCl(DAPTA)] (2).** A similar procedure to the synthesis of complex **1** was followed using DAPTA (0.17 mmol, 39.0 mg) as the phosphine ligand.

Yield = 86% (67.8 mg) based on the metal salt. Elemental analysis calcd (%) for $C_9H_{16}AuClN_3O_2P$: C 23.42, H 3.49, N 9.10; found: C 23.61, H 3.45, N 8.49. ATR-FTIR, $\nu$ ($cm^{-1}$): 2923 vw, 1633 s, 1416 m, 1354 m, 1332 m, 1228 m, 1208 m, 1126 w,

 

1097 w, 1047 m, 991 m, 890 m, 873 w, 796 m, 728 m, 702 m, 632 m. $^{1}$H NMR (400 MHz, DMSO-d$_6$), $\delta$ (ppm): 5.52 (d, 1H, $^{2}J_{HH}$ = 9.2 Hz, NC$H_2$N), 5.40 (dd, 1H, $^{2}J_{HP}$ = 10.2 Hz, $^{2}J_{HH}$ = 6.4 Hz, NC$H_2$P), 4.94–4.86 (m, {1H, NC$H_2$N}), ({1H, NC$H_2$P}), 4.63 (d, 1H, $^{2}J_{HH}$ = 9.2 Hz, NC$H_2$N), 4.30 (dt, 1H, $J_{HP}$ = 10.0 Hz, $J_{HH}$ = 2.0 Hz, PC$H_2$N), 4.11 (d, $^{2}J_{HH}$ = 8.8 Hz, NC$H_2$N), 4.04 (s, 2H, NC$H_2$P), 3.77 (dt, 1H, $J_{HP}$ = 10.0 Hz, $J_{HH}$ = 2.0 Hz, NC$H_2$P), 1.96 (s, 3H, COC$H_3$), 1.94 (s, 3H, COC$H_3$). $^{31}$P{$^{1}$H} NMR (400 MHz, DMSO-d$_6$), $\delta$ (ppm): −26.74. $^{13}$C{$^{1}$H} NMR (600 MHz, DMSO-d$_6$), $\delta$ (ppm): 169.41 (*C*OCH$_3$), 168.62 (*C*OCH$_3$), 66.58 (NCH$_2$N), 60.98 (NCH$_2$N), 54.94 (NCH$_2$N), 47.43 (d, $^{1}J_{PC}$ = 71.2 Hz, PCH$_2$N), 43.78 (d, $^{1}J_{PC}$ = 72.8 Hz, PCH$_2$N), 38.19 (d, $^{1}J_{PC}$ = 75,2 Hz, PCH$_2$N), 21.57 (COCH$_3$), 21.26 (COCH$_3$). DEPT (600 MHz, DMSO-d$_6$), $\delta$ (ppm): 66.32, 60.76, 47.17, 43.53, 37.94, 21.31, 21.01. MALDI-MS (DCTB matrix), *m*/*z* (assignment, % intensity): 484 ([M + Na]$^+$, 9), 461 ([M]$^+$, 1), 426 ([M − Cl]$^+$, <1).

**[AuCl(DBPTA)] (3).** The previous synthetic procedures were followed although using DBPTA (0.17 mmol, 60.1 mg). In this case, the colourless precipitate of the compound appeared only after the addition of *n*-pentane.

Yield = 77% (76.8 mg) based on the metal salt. Elemental analysis calcd (%) for $C_{19}H_{20}AuClN_3O_2P$: C 38.96, H 3.44, N 7.17; found: C 38.68, H 3.86, N 6.54. ATR-FTIR, $\nu$ (cm$^{-1}$): 3058 vw, 2956 vw, 2923 w, 2854 vw, 1631 s, 1578 w, 1529 w, 1489 w, 1446 w, 1407 m, 1336 m, 1242 m, 1125 w, 1075 m, 1002 m, 928 w, 900 w, 865 w, 789 w, 699 s, 657 w. $^{1}$H NMR (600 MHz, DMSO-d$_6$), $\delta$ (ppm): 7.51–7.44 (m, 10H, Ar–H), 5.36 (dd, 1H, $^{2}J_{HP}$ = 13.7 Hz, $^{2}J_{HH}$ = 11.9 Hz, NC$H_2$P), 5.19 (d, 1H, $^{2}J_{HH}$ = 13.7 Hz, NC$H_2$N), 4.89 (d, 1H, $^{2}J_{HH}$ = 13.3 Hz, NC$H_2$N), 4.66 (d, 1H, $^{2}J_{HH}$ = 12.6 Hz, NC$H_2$N), 4.57 (t, 1H, $^{2}J_{HH}$ = 11.9 Hz, NC$H_2$N), 4.40 (d, 1H, $^{2}J_{HH}$ = 14.4 Hz, NC$H_2$P), 4.30 (d, 1H, $^{2}J_{HH}$ = 13.7 Hz, NC$H_2$P), 4.07 (s, 3H, NC$H_2$P), 4.03 (d, 1H, $^{2}J_{HH}$ = 15.5 Hz, NC$H_2$P). $^{31}$P{$^{1}$H} NMR (400 MHz, DMSO-d$_6$), $\delta$ (ppm): −24.53. $^{13}$C{$^{1}$H} NMR (600 MHz, DMSO-d$_6$), $\delta$ (ppm): 169.98 (*C*OC$_6$H$_5$), 169.48 (*C*OC$_6$H$_5$), 134.64 ($C_{quat}$–CO), 134.57 ($C_{quat}$–CO), 130.19 (Ar–*C*H), 129.61 (Ar–*C*H), 128.55 (Ar–*C*H), 128.24 (Ar–*C*H), 128.13 (Ar–*C*H), 127.50 (Ar–*C*H), 68.21 (NCH$_2$N), 61.85 (NCH$_2$N), 46.83 (d, $^{1}J_{PC}$ = 108 Hz, PCH$_2$N), 45.33 (d, $^{1}J_{PC}$ = 128 Hz, PCH$_2$N), 38.65 (d, $^{1}J_{PC}$ = 128 Hz, PCH$_2$N). DEPT (600 MHz, DMSO-d$_6$), $\delta$ (ppm): 129.92, 129.65, 128.30, 127.98, 127.87, 127.24, 67.93, 61.62, 46.59, 45.09, 38.38. MALDI-MS (DCTB matrix), *m*/*z* (assignment, % intensity): 608 ([M + Na]$^+$, 3).

**[AuCl(PTA-CH$_2$-C$_6$H$_4$-*p*-COOH)]Br (4).** In a small flask equipped with a magnetic stirring bar, [AuCl(Me$_2$S)] (0.17 mmol, 50 mg) was dissolved in 4 mL of acetone. Solid (PTA-CH$_2$-C$_6$H$_4$-*p*-COOH)Br·H$_2$O (0.17 mmol, 66.3 mg) was then directly added and the obtained mixture was stirred overnight at r.t. The yellowish-colourless precipitate formed was washed with portions of diethyl ether (or *n*-pentane) and dried under vacuum.

Yield = 87% (88.7 mg) based on the metal salt. Elemental analysis calcd (%) for $C_{14}H_{19}AuBrClN_3O_2P$: C 27.81, H 3.17, N 6.95; found: C 27.16, H 3.31, N 6.52. ATR-FTIR, $\nu$ (cm$^{-1}$): 3316 br vw, 3260 br vw, 2961 w, 2918 w, 1698 br m, 1615 w, 1579 w, 1456 w, 1420 w, 1385 w, 1309 w, 1283 w, 1231 w, 1183 w, 1118 w, 1070 w, 1033 w, 988 w, 926 w, 900 w, 886 w, 855 w, 810 m, 753 m, 734 s, 699 w, 629 w. $^{1}$H NMR (400 MHz, DMSO-d$_6$, $\delta$)/COSY: 13.21 (br s, COO*H*), 8.08 (d, $^{3}J_{HH}$ = 5.2 Hz, 2H, Ar–H, C*H*–C–COOH), 7.68 (d, $^{3}J_{HH}$ = 5.2 Hz, Ar–H, 2H, C*H*–C–CH$_2$), 5.26 (d, $^{2}J_{HH}$ = 12 Hz, 2H, NC$H_2$N$^+$), 5.01 (d, $^{2}J_{HH}$ = 12 Hz, 2H, NC$H_2$N$^+$), 4.68 (d, 2H, $^{2}J_{HH}$ = 8 Hz, NC$H_2$N), 4.58 (d, $^{2}J_{HH}$ = 12 Hz, 1H, CC$H_2$N$^+$), 4.39–4.33 (m, {1H, CC$H_2$N$^+$}, {4H, PC$H_2$N}), 4.23 (d, $^{2}J_{HP}$ = 12 Hz, 2H, PC$H_2$N$^+$). $^{31}$P{$^{1}$H} NMR (400 MHz, DMSO-d$_6$), $\delta$ (ppm): −30.83. $^{13}$C{$^{1}$H} NMR (400 MHz, DMSO-d$_6$, $\delta$)/DEPT/HSQC: 166.86 (*C*OOH), 133.40 (*C*H–C–CH$_2$), 132.55 ($C_{quat}$–COOH), 129.83 ($C_{quat}$–CH$_2$), 129.78 (*C*H–C–COOH), 78.83 (d, *J* = 20 Hz, NC$H_2$N$^+$), 68.71 (d, *J* = 32 Hz, NC$H_2$N), 63.74 (CC$H_2$N$^+$), 51.01 (d, $^{1}J_{pc}$ = 84 Hz, PC$H_2$N$^+$), 47.48 (d, $^{1}J_{pc}$ = 92 Hz, PC$H_2$N). DEPT (400 MHz, DMSO-d$_6$, $\delta$): 133.16, 129.59, 78.58, 68.46, 63.49, 51.76, 47.24. MALDI-MS (DCTB matrix), *m*/*z* (assignment, % intensity): 604 ([M + H]$^+$, 4), 568 ([M − Cl]$^+$, 7).

**[AuCl(PTA-CH$_2$-C$_6$H$_3$-*p*-OH-*m*-CHO)]Cl (5).** A similar procedure to the synthesis of complex **4** was followed, but solid (PTA-CH$_2$-C$_6$H$_3$-*p*-OH-*m*-CHO)Cl (0.17 mmol, 55.7 mg) was added instead, yielding a light yellow precipitate.

Yield = 94% (88.8 mg) based on the metal salt. Elemental analysis calcd (%) for $C_{14}H_{19}AuCl_2N_3O_2P$: C 30.02, H 3.42, N 7.50; found: C 31.03, H 3.85, N 7.26. ATR-FTIR, $\nu$ (cm$^{-1}$): 2985 vw, 2919 vw, 2859 vw, 1687 m, 1661 m, 1614 w, 1490 w, 1446 w, 1420 w, 1382 w, 1356 w, 1305 w, 1292 w, 1250 w, 1213 w, 1154 w, 1119 w, 1065 w, 1031 w, 987 w, 950 w, 917 w, 897 w, 816 m, 743 m, 679 w, 623 w. $^{1}$H NMR (400 MHz, DMSO-d$_6$, $\delta$)/COSY: 11.44 (s, 1H, O*H*), 10.34 (s, 1H, C*H*O), 7.79 (s, 1H, Ar–H, C*H*–C–CHO), 7.65 (d, *J* = 8 Hz, 1H, Ar–H, CH–C*H*–C–CH$_2$), 7.24 (d, *J* = 8 Hz, 1H, Ar–H, C*H*–C–OH), 5.23 (d, *J* = 12 Hz, 2H, NC$H_2$N$^+$), 4.97 (d, *J* = 12 Hz, 2H, NC$H_2$N$^+$), 4.66 (d, *J* = 4 Hz, 2H, PC$H_2$N$^+$), 4.57 (d, *J* = 12 Hz, 1H, NC$H_2$N), 4.39–4.31 (m, {1H, NC$H_2$N}, {2H, CC$H_2$N$^+$}, {2H, PC$H_2$N}), 4.21 (d, *J* = 16 Hz, 2H, PC$H_2$N). $^{31}$P{$^{1}$H} NMR (400 MHz, DMSO-d$_6$, $\delta$): −32.71. $^{13}$C{$^{1}$H} NMR (400 MHz, DMSO-d$_6$, $\delta$)/DEPT/HSQC: 190.41 (*C*HO), 162.39 ($C_{quat}$–OH), 140.33 (*C*H–$C_{quat}$–CH$_2$), 133.31 (*C*H–C–CHO), 122.66 (*C*–CHO), 118.30 ($C_{quat}$–CH$_2$), 115.90 (*C*H–C–OH), 78.30 (d, *J* = 24 Hz, NC$H_2$N$^+$), 68.72 (d, *J* = 32 Hz, NC$H_2$N), 63.77 (CC$H_2$N$^+$), 51.59 (d, $^{1}J_{pc}$ = 88 Hz, PC$H_2$N$^+$), 47.44 (d, $^{1}J_{pc}$ = 88, PC$H_2$N). DEPT (400 MHz, DMSO-d$_6$, $\delta$): 190.15, 140.08, 133.05, 118.05, 78.05, 68.46, 63.51, 51.33, 47.19. MALDI-MS (DCTB matrix), *m*/*z* (assignment, % intensity): 582.33 ([M + Na]$^+$, 0.8), 559.34 ([M]$^+$, 1.2), 524.29 ([M − Cl]$^+$, 3.2).

### 4.3. Heterogenization of the Au(I) complexes in the carbon supports

Activated carbon (AC) Norit RO 0.8 from Sigma-Aldrich and multi-walled carbon nanotubes (CNT) NC3100 from Nanocyl were used in their original forms as-purchased. Their oxidized derivatives were prepared with the treatment using $HNO_3$ (AC-ox and CNT-ox) followed by NaOH (AC-ox-Na and CNT-ox-Na), according with the published procedures.[39,40]

The gold(I) complexes **1–5** were anchored onto different carbon materials (0.050 g) – AC, AC-ox, AC-ox-Na, CNT, CNT-ox and CNT-ox-Na. The required amount to achieve approximately 2% Au per mass of carbon (determined by ICP analysis) was weighed and dissolved in 8 mL of an acetonitrile/water

mixture (1 : 1). The samples were stirred at room temperature overnight, then separated by gravity filtration, washed with $CH_3CN/H_2O$ and dried overnight at 40 °C in an oven. The heterogenization process was monitored by UV/Vis spectroscopy: 3 mL aliquots of the solution were taken after 1, 4 or 24 h, analysed, and then returned to the solution.

### 4.4. Catalytic reactions

The peroxidative oxidation reactions were carried out in 10 mL capped glass tubes under vigorous stirring. A 1 : 1 mixture of acetonitrile and water (1.5 mL) was added to the solid Au(I) complexes (1.5 μmol) in an Eppendorf tube, which was dissolved in an ultrasonic bath before the addition of silver(I) triflate AgOTf (1.5 μmol for complexes **1–3**; 3 μmol for **4–5**). After centrifugation, the supernatant solution was transferred to the glass tube and acetonitrile (2.516 or 2.115 mL, when using $H_2O_2$ or TBHP, respectively), $CH_3NO_2$ [GC internal standard] (1.0 mmol; 0.541 mL of stock solution 1.85 M in $CH_3CN$), nitric acid (0.025 mmol; 0.050 mL of stock solution of $HNO_3$ 0.50 M in $CH_3CN$) and cyclohexane (1.0 mmol; 0.109 mL) were added in this order. The peroxide was then added dropwise (5.0 mmol; 0.284 mL of a 50% $H_2O_2$ aqueous solution or 0.685 mL of a 70% TBHP aqueous solution), and the reaction was typically left for 4 h at 50 °C. After quenching for at least 10 min with an excess of solid $PPh_3$, approximately 0.5 μL of the sample was directly analysed by GC. The products (cyclohexanol, CyOH, and cyclohexanone, Cy′O) were identified by comparing their retention times with those of authentic samples.

Concerning the experiments under MW irradiation, appropriate 10 mL reaction tubes, capable of being sealed, were employed. The protocol described above was followed, with modifications, including shorter reaction times (typically 0.5 h) and higher temperatures (50, 70 or 80 °C).

For the MW-assisted reactions using the supported Au(I) complexes, the supernatant solution from the Eppendorf tube was discarded. Then 2.865 mL of acetonitrile were added to the solid residue and the suspension was transferred to the G10 vial, followed by the sequential addition of $H_2O$ (0.750 mL), nitromethane, the promoter ($HNO_3$), cyclohexane and the tested oxidant (TBHP). At the end of the reaction, *ca.* 0.3 μL of the sample was directly analysed by GC.

### 4.5. Cytotoxicity assays

The cell lines (A2780, A2780*cis*, HCT116, A549, MRC-5) were cultured according to the supplier guidelines and maintained at 37 °C in a humidified atmosphere with 5% $CO_2$. In 96-well plates, $1 \times 10^3$ cancer cells (or $8 \times 10^3$ MRC-5 normal cells) were seeded and treated 24 hours later with six different concentrations of gold complexes **1–5** (0.001, 0.01, 0.1, 1, 10, 100 μM). Stock solutions (10 mM) of all digold complexes were prepared in DMSO as the solvent. After 96 h of treatment, cell viability was assessed using the CellTiter-Glo assay (Promega, Madison, WI, USA) with Tecan M1000 or SynergyH1 microplate readers. $IC_{50}$ values were calculated from logistical dose–response curves using GraphPad Prism software. All measurements were performed in triplicate, and averages with standard deviations are presented as error bars.

## Author contributions

Nuno Reis Conceição, Thomas Scattolin, Sónia A. C. Carabineiro, Armando J. L. Pombeiro: conception and design of study; Nuno Reis Conceição, Abdallah G. Mahmoud, Martin C. Dietl, Isabella Caligiuri, Matthias Rudolph, M. Fátima C. Guedes da Silva: acquisition of data; Nuno Reis Conceição, Abdallah G. Mahmoud, Martin C. Dietl, Isabella Caligiuri, Sónia A. C. Carabineiro, Matthias Rudolph, M. Fátima C. Guedes da Silva, Armando J. L. Pombeiro, Thomas Scattolin: analysis and/or interpretation of data; Nuno Reis Conceição, Abdallah G. Mahmoud, Sónia A. C. Carabineiro, Thomas Scattolin, Flavio Rizzolio, Armando J. L. Pombeiro, A. Stephen K. Hashmi: project management, fund acquisition, writing, review, and editing.

## Data availability

The datasets supporting this article have been uploaded as part of the ESI.†

## Conflicts of interest

There are no conflicts to declare.

## Acknowledgements

Centro de Química Estrutural (CQE) acknowledges the financial support of Fundação para a Ciência e Tecnologia (FCT) through projects UIDB/00100/2020 (DOI: 10.54499/UIDB/00100/2020), UIDP/00100/2020 (DOI: 10.54499/UIDP/00100/2020), and LA/P/0056/2020 (DOI: 10.54499/LA/P/0056/2020). N. R. C. acknowledges the financial support from Research fellowship BL2/2020_IST-ID of CQE (project 1801P.00974.1.01.01, UIDB/00100/2020) and Programa Doutoral FCT ''Catalysis and Sustainability'' (PD/00248/2012). A. G. M. acknowledges FCT for the international call of Scientific Employment Stimulus (2023.06724.CEECIND) DOI: 10.54499/2023.06724.CEECIND/CP2836/CT0005. FCT/MCTES is also acknowledged for projects DOIs: 10.54499/LA/P/0008/2020, 10.54499/UIDB/50006/2020 and 10.54499/UIDP/50006/2020 (LAQV), and bilateral project Portugal-Germany 5625-DRI-DAAD-2020/21. S. A. C. C. also acknowledges FCT for the Scientific Employment Stimulus – Institutional Call (DOI: 10.54499/CEECINST/00102/2018/CP1567/CT0026). Concerning the biological part, this research was funded by Fondazione AIRC per la Ricerca sul Cancro, IG23566. We acknowledge the supervision of Dr J. Gross for the HR-MS experiments conducted at the Chemistry Department of Heidelberg University.

 

## References


1 M. Rudolph and A. S. K. Hashmi, *Chem. Soc. Rev.*, 2012, **41**, 2448–2462.
2 D. Pflästerer and A. S. K. Hashmi, *Chem. Soc. Rev.*, 2016, **45**, 1331–1367.
3 C. M. Hendrich, K. Sekine, T. Koshikawa, K. Tanaka and A. S. K. Hashmi, *Chem. Rev.*, 2021, **121**, 9113–9163.
4 A. S. K. Hashmi, *Nature*, 2007, **449**, 292–293.
5 C. Zhang, K. Hong, C. Pei, S. Zhou, W. Hu, A. S. K. Hashmi and X. Xu, *Nat. Commun.*, 2021, **12**, 1–11.
6 C. Hu, T. Wang, M. Rudolph, T. Oeser, A. M. Asiri and A. S. K. Hashmi, *Angew. Chem., Int. Ed.*, 2020, **59**, 8522–8526.
7 Q. Wang, S. Hoffmann, J. Schießl, M. Rudolph, F. Rominger and A. S. K. Hashmi, *Eur. J. Org. Chem.*, 2020, 2384–2388.
8 E. N. Kolobova, E. G. Pakrieva, S. A. C. Carabineiro, N. Bogdanchikova, A. N. Kharlanov, S. O. Kazantsev, J. Hemming, P. Mäki-Arvela, A. N. Pestryakov and D. Y. Murzin, *Green Chem.*, 2019, **21**, 3370–3382.
9 E. Pakrieva, E. Kolobova, G. Mamontov, N. Bogdanchikova, M. H. Farias, L. Pascual, V. Cortés Corberán, S. Martinez Gonzalez, S. A. C. Carabineiro and A. Pestryakov, *ChemCatChem*, 2019, **11**, 1615–1624.
10 S. A. C. Carabineiro, A. P. C. Ribeiro, J. G. Buijnsters, M. Avalos-Borja, A. J. L. Pombeiro, J. L. Figueiredo and L. M. D. R. S. Martins, *Catal. Today*, 2020, **357**, 22–31.
11 E. Kolobova, P. Mäki-Arvela, A. Grigoreva, E. Pakrieva, S. A. C. Carabineiro, J. Peltonen, S. Kazantsev, N. Bogdanchikova, A. Pestryakov and D. Y. Murzin, *Catal. Today*, 2021, **367**, 95–110.
12 I. L. Librando, A. G. Mahmoud, S. A. C. Carabineiro, M. F. C. G. da Silva, F. J. Maldonado-Hódar, C. F. G. C. Geraldes and A. J. L. Pombeiro, *Catalysts*, 2022, **12**, 45.
13 M. P. deAlmeida and S. A. C. Carabineiro, *ChemCatChem*, 2012, **4**, 18–29.
14 X. Z. Shu, S. C. Nguyen, Y. He, F. Oba, Q. Zhang, C. Canlas, G. A. Somorjai, A. P. Alivisatos and F. D. Toste, *J. Am. Chem. Soc.*, 2015, **137**, 7083–7086.
15 G. Beaton, J. Zacks and K. Stamplecoskie, *Colloids Surf., A*, 2022, **646**, 128972.
16 L. Xuan Dien, T. Murayama, N. Tuan Hung, Q. Duc Truong, H. Dang Chinh, M. Yoshimura, M. Haruta and T. Ishida, *J. Catal.*, 2022, **408**, 236–244.
17 S. Kramer, N. R. Bennedsen and S. Kegnæs, *ACS Catal.*, 2018, **8**, 6961–6982.
18 J. He, C. Lai, L. Qin, B. Li, S. Liu, L. Jiao, Y. Fu, D. Huang, L. Li, M. Zhang, X. Liu, H. Yi, L. Chen and Z. Li, *Chemosphere*, 2020, **256**, 127083.
19 J. Wolska, A. Walkowiak, I. Sobczak, L. Wolski and M. Ziolek, *Catal. Today*, 2021, **382**, 48–60.
20 C. Y. Sun, W. P. To, X. L. Wang, K. T. Chan, Z. M. Su and C. M. Che, *Chem. Sci.*, 2015, **6**, 7105–7111.
21 V. A. Levchenko, H. S. M. Siah, S. Øien-Ødegaard, G. Kaur, A. Fiksdahl and M. Tilset, *Mol. Catal.*, 2020, **492**, 111009.
22 R. Boppella, J. Tan, W. Yang and J. Moon, *Adv. Funct. Mater.*, 2019, **29**, 1807976.
23 I. L. Librando, A. Paul, A. G. Mahmoud, A. V. Gurbanov, S. A. C. Carabineiro, F. C. Guedes da Silva, C. F. G. C. Geraldes and A. J. L. Pombeiro, *RSC Sustainability*, 2023, **1**, 147–158.
24 A. G. Mahmoud, I. L. Librando, A. Paul, S. A. C. Carabineiro, A. M. Ferraria, A. M. Botelho do Rego, M. F. C. Guedes da Silva, C. F. G. C. Geraldes and A. J. L. Pombeiro, *Catal. Today*, 2023, **423**, 114270.
25 M. P. De Almeida, L. M. D. R. S. Martins, S. A. C. Carabineiro, T. Lauterbach, F. Rominger, A. S. K. Hashmi, A. J. L. Pombeiro and J. L. Figueiredo, *Catal. Sci. Technol.*, 2013, **3**, 3056–3069, DOI: **10.1039/c3cy00552f**.
26 S. A. C. Carabineiro, L. M. D. R. S. Martins, A. J. L. Pombeiro and J. L. Figueiredo, *ChemCatChem*, 2018, **10**, 1804–1813.
27 C. Vriamont, M. Devillers, O. Riant and S. Hermans, *Chem. Commun.*, 2013, **49**, 10504–10506.
28 C. Vriamont, M. Devillers, O. Riant and S. Hermans, *Chem. – Eur. J.*, 2013, **19**, 12009–12017.
29 D. Ventura-Espinosa, S. Sabater and J. A. Mata, *J. Catal.*, 2017, **352**, 498–504.
30 A. G. Mahmoud, M. F. C. Guedes da Silva and A. J. L. Pombeiro, *Coord. Chem. Rev.*, 2021, **429**, 213614.
31 A. G. Mahmoud, M. F. C. Guedes da Silva and A. J. L. Pombeiro, *Catal. Today*, 2023, **418**, 114056.
32 A. G. Mahmoud, M. F. C. Guedes da Silva and P. Smoleński, Insights into Copper Complexes of PTA and Related Ligands: Synthesis, Structural Features and Applications, in *Synthesis and Applications in Chemistry and Materials*, ed. A. J. L. Pombeiro, World Scientific Publishing Company, 2024, pp. 77–106.
33 A. G. Mahmoud, J. V. Nardeli, M. J. Ferreira, A. M. Ferraria, A. M. Botelho do Rego, M. F. C. Guedes da Silva and A. J. L. Pombeiro, *Batteries Supercaps*, 2023, e202300564.
34 A. Guerriero and L. Gonsalvi, *Inorg. Chim. Acta*, 2024, **572**, 122295.
35 A. G. Mahmoud, M. F. C. Guedes da Silva, J. Sokolnicki, P. Smoleński and A. J. L. Pombeiro, *Dalton Trans.*, 2018, **47**, 7290–7299.
36 A. G. Mahmoud, M. F. C. Guedes da Silva, E. I. Śliwa, P. Smoleński, M. L. Kuznetsov and A. J. L. Pombeiro, *Chem. – Asian J.*, 2018, **13**, 2868–2880.
37 A. G. Mahmoud, P. Smolénski, M. F. C. Guedes Da Silva and A. J. L. Pombeiro, *Molecules*, 2020, **25**, 5479.
38 A. G. Mahmoud, M. F. C. Guedes da Silva and A. J. L. Pombeiro, *Dalton Trans.*, 2021, **50**, 6109–6125.
39 I. L. Librando, A. G. Mahmoud, S. A. C. Carabineiro, M. F. C. Guedes da Silva, C. F. G. C. Geraldes and A. J. L. Pombeiro, *Catalysts*, 2021, **11**, 185.
40 I. L. Librando, A. G. Mahmoud, S. A. C. Carabineiro, M. F. C. Guedes da Silva, C. F. G. C. Geraldes and A. J. L. Pombeiro, *Nanomaterials*, 2021, **11**, 2702.
41 N. Reis Conceição, A. G. Mahmoud, M. F. C. Guedes da Silva, K. T. Mahmudov and A. J. L. Pombeiro, *Mol. Catal.*, 2023, **549**, 113512.
42 A. Bergamo, P. J. Dyson and G. Sava, *Coord. Chem. Rev.*, 2018, **360**, 17–33.
43 I. Ott, *Adv. Inorg. Chem.*, 2020, **75**, 121–148.

44 N. J. Wheate, S. Walker, G. E. Craig and R. Oun, *Dalton Trans.*, 2010, **39**, 8113–8127.
45 A. Gatti, A. Habtemariam, I. Romero-Canelón, J. I. Song, B. Heer, G. J. Clarkson, D. Rogolino, P. J. Sadler and M. Carcelli, *Organometallics*, 2018, **37**, 891–899.
46 Y. A. Vorotnikov, N. A. Vorotnikova and M. A. Shestopalov, *Materials*, 2023, **16**, 5869.
47 T. Scattolin, V. A. Voloshkin, F. Visentin and S. P. Nolan, *Cell Rep. Phys. Sci.*, 2021, **2**, 100446.
48 T. Scattolin, I. Pessotto, E. Cavarzerani, V. Canzonieri, L. Orian, N. Demitri, C. Schmidt, A. Casini, E. Bortolamiol, F. Visentin, F. Rizzolio and S. P. Nolan, *Eur. J. Inorg. Chem.*, 2022, e202200103.
49 L. Messori and G. Marcon, Gold Complexes in the Treatment of Rheumatoid Arthritis, in *Metal ions in biological systems*, ed. A. Sigel and H. Sigel, Marcel Dekker Inc., New York, 2004, pp. 279–304.
50 T. Zou, C. T. Lum, C. N. Lok, J. J. Zhang and C. M. Che, *Chem. Soc. Rev.*, 2015, **44**, 8786–8801.
51 J. J. Zhang, M. A. Abu el Maaty, H. Hoffmeister, C. Schmidt, J. K. Muenzner, R. Schobert, S. Wölfl and I. Ott, *Angew. Chem., Int. Ed.*, 2020, **59**, 16795–16800.
52 S. M. Meier-Menches, B. Neuditschko, K. Zappe, M. Schaier, M. C. Gerner, K. G. Schmetterer, G. Del Favero, R. Bonsignore, M. Cichna-Markl, G. Koellensperger, A. Casini and C. Gerner, *Chem. – Eur. J.*, 2020, **26**, 15528–15537.
53 T. A. C. A. Bayrakdar, T. Scattolin, X. Ma and S. P. Nolan, *Chem. Soc. Rev.*, 2020, **49**, 7044–7100.
54 J. R. Stenger-Smith and P. K. Mascharak, *ChemMedChem*, 2020, **15**, 2136–2145.
55 C. Schmidt, L. Albrecht, S. Balasupramaniam, R. Misgeld, B. Karge, M. Brönstrup, A. Prokop, K. Baumann, S. Reichl and I. Ott, *Metallomics*, 2019, **11**, 533–545.
56 C. Schmidt, B. Karge, R. Misgeld, A. Prokop, R. Franke, M. Brönstrup and I. Ott, *Chem. – Eur. J.*, 2017, **23**, 1869–1880.
57 C. K. Mirabelli, R. K. Johnson, C. M. Sung, L. Faucette, K. Muirhead and S. T. Crooke, *Cancer Res.*, 1985, **45**, 32–39.
58 G. X. Hou, P. P. Liu, S. Zhang, M. Yang, J. Liao, J. Yang, Y. Hu, W. Q. Jiang, S. Wen and P. Huang, *Cell Death Dis.*, 2018, **9**, 1–15.
59 B. Kemper, Y. R. Hristova, S. Tacke, L. Stegemann, L. S. Van Bezouwen, M. C. A. Stuart, J. Klingauf, C. A. Strassert and P. Besenius, *Chem. Commun.*, 2015, **51**, 5253–5256.
60 E. Vergara, S. Miranda, F. Mohr, E. Cerrada, E. R. T. Tiekink, P. Romero, A. Mendía and M. Laguna, *Eur. J. Inorg. Chem.*, 2007, 2926–2933.
61 E. Atrián-Blasco, S. Gascón, M. J. Rodríguez-Yoldi, M. Laguna and E. Cerrada, *Eur. J. Inorg. Chem.*, 2016, 2791–2803.
62 F. Maia, N. Mahata, B. Jarrais, A. R. Silva, M. F. R. Pereira, C. Freire and J. L. Figueiredo, *J. Mol. Catal. A: Chem.*, 2009, **305**, 135–141.
63 M. Sutradhar, L. M. D. R. S. Martins, S. A. C. Carabineiro, M. F. C. Guedes da Silva, J. G. Buijnsters, J. L. Figueiredo and A. J. L. Pombeiro, *ChemCatChem*, 2016, **8**, 2254–2266.
64 L. M. D. R. S. Martins, A. P. C. Ribeiro, S. A. C. Carabineiro, J. L. Figueiredo and A. J. L. Pombeiro, *Dalton Trans.*, 2016, **45**, 6816–6819.
65 D. Dey, A. Al-Hunaiti, V. Gopal, B. Perumalsamy, G. Balakrishnan, T. Ramasamy, D. Dharumadurai and B. Biswas, *J. Mol. Struct.*, 2020, **1222**, 128919.
66 S. A. C. Carabineiro, L. M. D. R. S. Martins, M. Avalos-Borja, J. G. Buijnsters, A. J. L. Pombeiro and J. L. Figueiredo, *Appl. Catal., A*, 2013, **467**, 279–290.
67 T. F. S. Silva, E. C. B. A. Alegria, L. M. D. R. S. Martins and A. J. L. Pombeiro, *Adv. Synth. Catal.*, 2008, **350**, 706–716.
68 C. Di Nicola, F. Garau, Y. Y. Karabach, L. M. D. R. S. Martins, M. Monari, L. Pandolfo, C. Pettinari and A. J. L. Pombeiro, *Eur. J. Inorg. Chem.*, 2009, 666–676.
69 T. F. S. Silva, G. S. Mishra, M. F. Guedes da Silva, R. Wanke, L. M. D. R. S. Martins and A. J. L. Pombeiro, *Dalton Trans.*, 2009, 9207.
70 M. N. Kopylovich, A. C. C. Nunes, K. T. Mahmudov, M. Haukka, T. C. O. Mac Leod, L. M. D. R. S. Martins, M. L. Kuznetsov and A. J. L. Pombeiro, *Dalton Trans.*, 2011, **40**, 2822–2836.
71 R. R. Fernandes, J. Lasri, M. F. C. G. Da Silva, J. A. L. Da Silva, J. J. R. Fraústo Da Silva and A. J. L. Pombeiro, *Appl. Catal., A*, 2011, **402**, 110–120.
72 N. Reis Conceição, B. P. Nobre, A. V. Gurbanov, A. M. F. Palavra, M. F. C. Guedes Da Silva, K. T. Mahmudov and A. J. L. Pombeiro, *Inorganics*, 2023, **11**, 62.
73 G. B. Shul'Pin, A. E. Shilov and G. Süss-Fink, *Tetrahedron Lett.*, 2001, **42**, 7253–7256.
74 A. M. Kirillov, M. V. Kirillova and A. J. L. Pombeiro, *Coord. Chem. Rev.*, 2012, **256**, 2741–2759.
75 M. A. Malik, A. A. Hashmi, A. S. Al-Bogami and M. Y. Wani, *J. Mater. Chem. B*, 2023, **12**, 552–576.
76 H. A. Khan, A. A. Isab, A. S. Alhomida, M. K. Gatasheh, A. R. Alhoshani, B. A. Aldhafeeri and N. R. Prasad, *Anti-Cancer Agents Med. Chem.*, 2024, **24**, 379–388.
77 Q. Cui, W. Ding, B. Luo, W. Lu, P. Huang and S. Wen, *Bioorg. Med. Chem.*, 2024, **112**, 117897.
78 J. G. Mehtala, S. Torregrosa-Allen, B. D. Elzey, M. Jeon, C. Kim and A. Wei, *Nanomedicine*, 2014, **9**, 1939–1955.
79 N. A. Yusoh, H. Ahmad and M. R. Gill, *ChemMedChem*, 2020, **15**, 2121–2135.
80 M. Yang, A. J. Pickard, X. Qiao, M. J. Gueble, C. S. Day, G. L. Kucera and U. Bierbach, *Inorg. Chem.*, 2015, **54**, 3316–3324.
81 X. Pan and X. Bao, *Acc. Chem. Res.*, 2011, **44**, 553–562.
82 S. Gu, A. N. Marianov and Y. Jiang, *Appl. Catal., B*, 2021, **300**, 120750.
83 D. J. Daigle, T. J. Decuir, J. B. Robertson and D. J. Darensbourg, 1,3,5-Triaz-7-Phosphatricyclo[3.3.1.1$^{3,7}$]Decane and Derivatives, in *Inorganic Syntheses*, ed. M. Y. Darensbourg, John Wiley & Sons, Ltd, 1998, pp. 40–45.
84 D. J. Darensbourg, C. G. Ortiz and J. W. Kamplain, *Organometallics*, 2004, **23**, 1747–1754.
85 A. Cervantes-Reyes, F. Rominger, M. Rudolph and A. S. K. Hashmi, *Chem. – Eur. J.*, 2019, **25**, 11745–11757.

 